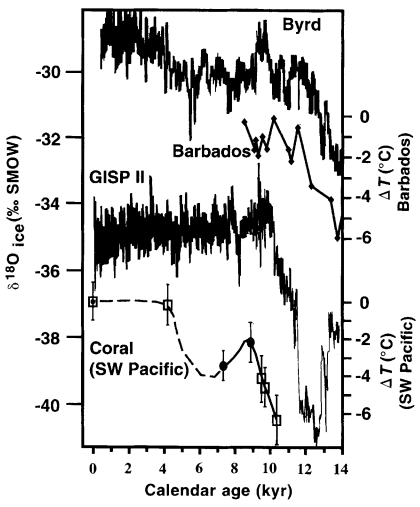


**Figure 2** Comparison of the coral Sr/Ca SST records from the SW Pacific (Vanuatu, open rectangles; New Guinea[31], filled ovals) with that from Barbados[3] (filled diamonds), and the $\delta^{18}O_{ice}$ records from the Greenland GISP II[1] and Antarctic Byrd[35] high-latitude ice cores. Coral data are plotted as deviation of mean annual SST from modern values. Error bars indicate the 1 s.d. annual range in mean monthly temperature variations for each 4–6 year period sampled. Note the extremely abrupt and rapid rise in SST between ~10.4 and 8.9 kyr BP in the SW Pacific record. Using a conversion[36] between temperature and $\delta^{18}O_{ice}$ of ~0.6‰ per °C for the ice cores, the changes in high-latitude atmospheric temperature in this time frame are comparable to the changes in SST observed in the tropical records.

coral SST reconstruction[3] also indicates a rapid 6 °C SST rise in the western equatorial Atlantic during the late deglaciation, the timing appears to be phase-shifted with that seen in the southwest Pacific by nearly 3 kyr, with most of the Atlantic warming occurring between 14 and 11.5 kyr BP (Fig. 2). We note that a similar phase shift in high-latitude deglacial warming has also recently been determined[35] based on a comparison of the GISP II and Byrd polar ice cores (Fig. 2). In that case, however, the inter-hemispheric phasing is reversed, with warming in the Antarctic beginning ~3 kyr before the warm Bølling period in Greenland. As seen in Fig. 2, the large rise in SST observed in the southwest Pacific much more closely matches the timing of the post-Younger Dryas warming seen in the GISP II record than in the Antarctic Byrd ice-core record. Nevertheless, the Byrd $\delta^{18}O$ record appears to mimic the southwest Pacific coral SST data after ~9 kyr BP. Although it is somewhat premature to extrapolate the entire deglacial climate from these four sites, these records appear to reveal a very surprising bipolar structure to the deglacial climate and suggest that strong meridional temperature gradients were maintained during parts of the last deglaciation. □

Received 22 November 1996; accepted 6 January 1997.

1. Alley, R. B. *et al. Nature* **362,** 527–529 (1993).
2. Fairbanks, R. G. *Paleoceanography* **5,** 937–948 (1990).
3. Guilderson, T. P., Fairbanks, R. & Rubenstone, J. L. *Science* **263,** 663–665 (1994).
4. CLIMAP Project Members *Seasonal Reconstructions of the Earth's Surface at the Last Glacial Maximum* (Map and Chart Ser., MC-36, Geol. Soc. Am., 1981).
5. Shackleton, N. J. *Quat. Sci. Rev.* **6,** 183–190 (1987).
6. Broecker, W. S. *Quat. Res.* **26,** 121–134 (1986).
7. Hope, G. S., Peterson, J. A., Radok, U. & Allison, I. *The Equatorial Glaciers of New Guinea* (Balkerma, Rotterdam, 1976).
8. Broecker, W. & Denton, G. S. *Geochim. Cosmochim. Acta* **53,** 305–341 (1989).
9. Thompson, L. G. *et al. Science* **269,** 46–50 (1995).
10. Rind, D. & Peteet, D. *Quat. Res.* **24,** 1–22 (1985).
11. Manabe, S. & Broccoli, A. J. *J. Atmos. Sci.* **42,** 2643–2651 (1985).
12. Hope, G. S. *J. Ecol.* **64,** 627–664 (1976).
13. Stute, M. *et al. Eos* **75,** 381 (1994).
14. Wright, H. E. Jr in *The Geology of North America: An Overview* (eds Bally, A. W. & Palmer, A. R.) 513–536 (Geol. Soc. Am., Boulder, 1989).
15. Palmer, T. N. & Mansfield, D. A. *Nature* **333,** 367–369 (1984).
16. Bony, S., Duvel, J.-P. & Treut, H. L. *Clim. Dynam.* **11,** 307–320 (1995).
17. Rind, D. *Nature* **346,** 317–318 (1990).
18. Walser, D. E. & Grahm, N. E. *J. Geophys. Res.* **96,** 12881–12893 (1993).
19. Schneider, N., Barnett, T., Latif, M. & Stockdale, T. *J. Clim.* **9,** 219–239 (1996).
20. Kutzbach, J. E., Guetter, P. J., Behling, P. J. & Selin, R. in *Global Climates since the Last Glacial Maximum* (ed. Wright, H. E. Jr) 24–93 (Univ. Minnesota Press, Minneapolis, 1993).
21. Beck, J. W. *et al. Science* **257,** 644–647 (1992).
22. McCulloch, M. T., Gagan, M. K., Mortimer, G. E., Chivas, A. R. & Isdale, P. *Geochim. Cosmochim. Acta* **58,** 2747–2754 (1994).
23. Shen, C. C. *et al. Geochim. Cosmochim. Acta* **60,** 3849–3858 (1996).
24. de Villiers, S., Shen, G. T. & Nelson, B. K. *Geochim. Cosmochim. Acta* **58,** 197–208 (1994).
25. Edwards, R. L., Chen, J. H. & Wasserburg, G. J. *Earth Planet. Sci. Lett.* **81,** 175–192 (1987).
26. Edwards, R. L. *et al. Science* **260,** 962–968 (1993).
27. Beck, W. *Science* **264,** 891 (1994).
28. Halpert, M. S. & Ropelewski, C. F. (NOAA, US Dept of Commerce, Silver Spring, MD, 1989).
29. Weber, J. N. & Woodhead, M. J. *J. Geophys. Res.* **77,** 463–473 (1972).
30. McConnaughey, T. *Geochim. Cosmochim. Acta* **53,** 151–162 (1989).
31. McCulloch, M. T. *et al. Earth Planet. Sci. Lett.* **138,** 169–178 (1996).
32. Martinez, J. I. *Palaeogeogr. Palaeoclimatol. Palaeoecol.* **112,** 19–62 (1994).
33. Harrison, S. & Dodson, J. in *Global Climates since the Last Glacial Maximum* (ed. Wright, H. E. Jr) 265–293 (Univ. Minnesota Press, Minneapolis, 1992).
34. Ruddiman, W. F. & Mix, A. C. in *Global Climates since the Last Glacial Maximum* (ed. Wright, H. E. Jr) 94–124 (Univ. Minnesota Press, Minneapolis, 1993).
35. Sowers, T. & Bender, M. *Science* **269,** 210–214 (1995).
36. Stuiver, M., Grootes, P. M. & Braziunas, T. F. *Quat. Res.* **44,** 341–354 (1995).
37. Alibert, C. & McCulloch, M. T. *Paleoceanography* (in the press).

**Acknowledgements.** We thank Th. Delcroix, A. Dessier, Ch. Henin and P. Rual for providing instrumental records of climate from New Caledonia, and S. Gray for providing one of the U/Th coral dates quoted here. This work was supported by ORSTOM (Institut Franç de Recherche Scientifique pour le Développement en Coopération), the US NSF and NOAA.

Correspondence should be addressed to J.W.B. (e-mail: wbeck@physics.arizona.edu).

# Interhemispheric synchrony of the last deglaciation inferred from alkenone palaeothermometry

**Edouard Bard*†, Frauke Rostek* & Corinne Sonzogni***

** CEREGE, Université d'Aix-Marseille III et CNRS-UMR 132, Europôle de l'Arbois, BP 80, 13545 Aix-en-Provence cedex 4, France*
*† Institut Universitaire de France*

**The relative timings of the last deglacial warming in the Southern and Northern hemispheres are not well constrained, but are a crucial component in understanding the mechanisms of deglaciation[1]. A clearer picture of the degree of interhemispheric synchrony has been obscured by a dearth of high-resolution temperature records that can be tied to the absolute calendar timescale. Moreover, the quantification of tropical temperatures during the last glacial cycle is controversial[2–8]. Here we apply the alkenone method of sea surface temperature reconstruction[9,10] to several high-resolution sediment cores recovered from the tropical Indian Ocean between 20° N and 20° S. The inferred initial sea surface temperature warming ~15,000 calendar years ago at 20° S is in phase with Northern Hemisphere sea (this study) and air[11] temperature changes, but lags Antarctic warming[12–14] by several millennia. This finding, along with the results of recent modelling studies[15,16], provides strong support for the idea that changes in the ocean's global thermohaline circulation were not the only cause of interhemispheric climate teleconnection during the last deglaciation.**

For high latitudes, the clearest palaeotemperature records are obtained from Greenland and Antarctica because amplitudes of climate variations were enhanced at high latitudes and because ice cores provide information at very high resolution for at least the last glacial cycle[11–14]. Although the exact relationship between atmospheric temperature and $\delta^{18}O$ in ice is still uncertain[17], there

is no doubt that very large temperature shifts of 6–10 °C were experienced in polar regions during the last glacial cycle.

For the low-latitude ocean, temperature variations during the last deglaciation have been evaluated by means of strontium measurements in corals[3]. However, the amplitude of the deglacial warming estimated from corals (5–6 °C) is in conflict with reconstructions based on micropalaeontological transfer functions which indicate almost no warming in the tropical belt between the Last Glacial Maximum (LGM) and the Holocene epoch[4]. Palaeotemperatures estimated by the transfer-function method are supported by the use of the modern analogue technique[5,6]. Small (<3 °C) temperature changes were also inferred from $\delta^{18}O$ measurements of planktonic foraminifera[7] (see also ref. 8 for recent work based on $\delta^{18}O$ analysis of single foraminifera).

The alkenone time series presented here are expressed in terms of $U^{K'}_{37}$ units, the simplified unsaturation index of C37 alkenones[10]. Gas chromatographic techniques used at CEREGE to quantify alkenones are described elsewhere[18]. Standard deviations better than 0.01 $U^{K'}_{37}$ units were obtained on replicated measurements of several deep sea sediment samples and an algal extract[18]. The $U^{K'}_{37}$ values have also been converted into sea surface temperature (SST) by applying a widely used calibration based on a coccolithophorids culture[19] (slope of 0.034 $U^{K'}_{37}$ units per °C). Although cultured prymnesiophyte strains display more than one response curve[20,21], several subsequent studies of natural samples (such as particulate, sediment-trap and core-top organic matter) have confirmed the usefulness of the original Prahl *et al.*[19] calibration for the SST range between 5 and 25 °C (refs 10, 18, 22, 23). In addition, recent work based on Indian Ocean core tops suggests that the slope of the $U^{K'}_{37}$ versus SST relationship could be smaller (0.023; ref. 18) above 24 °C than observed for the 5–25 °C range. Although a firm confirmation using cultures is needed, this possibility must be kept in mind when evaluating amplitudes of temperature changes.

Figure 1a and b presents the $\delta^{18}O$ and $U^{K'}_{37}$ time series obtained on cores MD85674 (3° 11′ N, 50° 26′ E, 4,875 m depth) and MD85668 (0° 01′ S, 46° 02′ E, 4,020 m depth). As can be clearly seen, the $\delta^{18}O$ records are unambiguous and there is little uncertainty on the assignments of isotope stages (see refs 24, 25 for MD85668 and 25, 26 for MD85674). Although the time resolution in core MD85674 is better than in core MD85668, the two alkenone records are highly similar and follow closely the $\delta^{18}O$ records measured in the two cores. The oxygen-isotope signal is mostly global in origin because the glacial/Holocene difference attributable to continental ice-volume changes is ~1.25‰, that is, 70–80% of the total $\delta^{18}O$ amplitude observed in the two cores. Moreover, there are striking similarities between the alkenone records and the isotopic temperatures from the Vostok site in Antarctica[27] (Fig. 1c). These facts clearly indicate that the last glacial cycle at the Indian Ocean Equator was dominated by global climate variations. In both deep sea cores, the maximum temperature is reached during isotopic substage 5e (the last interglacial period at ~125,000 calendar years before present, cal. yr BP) while cold minima correspond to isotopic stage 4 and stage 2 (LGM at ~20,000 cal. yr BP). The total amplitude change is of the order of 2.5–3 °C for the whole glacial cycle and only 1.5 °C for the transition between LGM and Holocene. The rather small deglacial warming observed for these two cores is typical of the equatorial-tropical zone of the Indian Ocean, as determined in 19 cores (Fig. 2) characterized by high sedimentation rates (usually >10 cm kyr$^{-1}$) and detailed $\delta^{18}O$ stratigraphies[26,28,29]. The mean deglacial warming based on the alkenone method is 1.7 °C ($1\sigma = 0.7$ °C) in broad agreement with previous work on foraminifera[5] (see Fig. 2) but significantly lower than the dramatic 5–6 °C deglacial warming inferred from the Sr/Ca ratio in tropical corals[3]. This conclusion remains valid (mean deglacial warming ~2.4 °C) when assuming a smaller slope of the $U^{K'}_{37}$ versus SST relationship for the high-temperature range (~0.023 instead of 0.034).

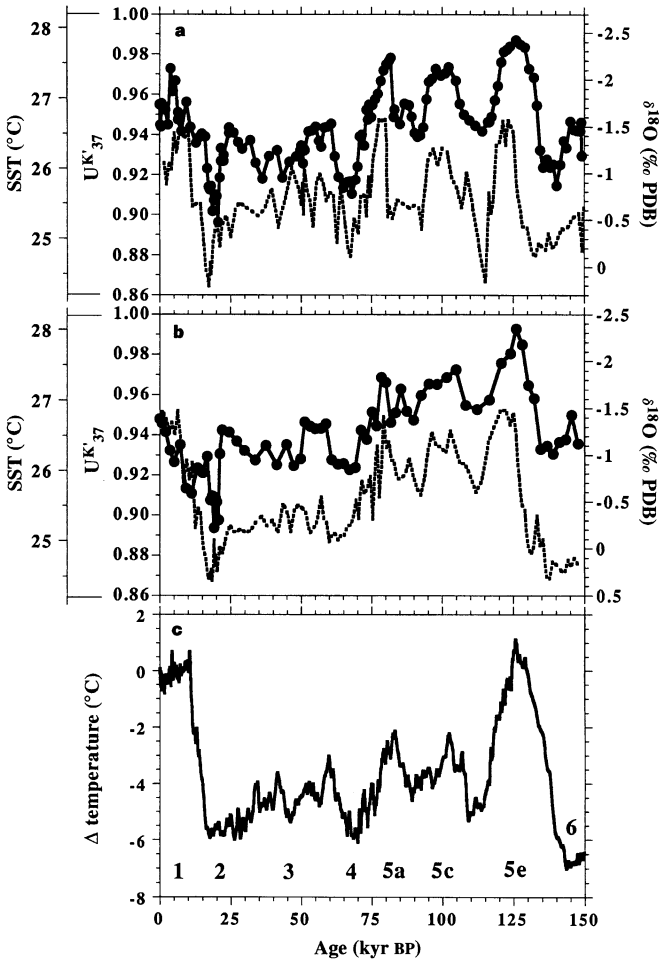


**Figure 1 a**, Solid line with dots, $U^{K'}_{37}$ record for core MD85674; dashed line, $\delta^{18}O$ record obtained on the bulk carbonate (data from ref. 26 and age-depth stratigraphy from ref. 25). **b**, Solid line with dots, $U^{K'}_{37}$ record for core MD85668; dashed line, $\delta^{18}O$ record obtained on the bulk carbonate (data and age-depth stratigraphy from ref. 24). The temperature calibration used to construct the SST *y*-axis is $U^{K'}_{37} = 0.034 \times SST + 0.039$ (ref. 19). The age-depth stratigraphies of the two cores are based on matching with the SPECMAP timescale with an average error of ~5 kyr. Nevertheless, the SST changes often lead by a few millennia the $\delta^{18}O$ variations observed in the same core. **c**, Smoothed temperature changes calculated for the Vostok site in Antarctica[27]. These relative temperature changes are calculated by assuming a deuterium/temperature gradient of 9‰ per °C after accounting for the isotopic change of sea water[27]. The record is corrected for the influence of the geographical position of the precipitation site[27] and the timescale is obtained by orbital tuning[38].

To describe in more detail the last deglaciation in the Southern Hemisphere, we show in Fig. 3a the complete alkenone record obtained for one core: MD79257, 20° 24′ S, 36° 20′ E, 1,260 m depth. This particular core has been precisely dated[29] by accelerator mass spectrometry $^{14}C$, so it is then possible to study the last deglaciation on an absolute timescale through the use of $^{14}C$ calibration formulas[30]. The LGM/Holocene temperature contrast is of the order of 2.5 °C which is at the high end of the set of 19 cores. The last deglaciation is characterized by an abrupt 1.5 °C warming at ~15,100 cal. yr BP followed by a transitory pause until ~12,200 cal. yr BP and a small cooling until ~11,500 cal. yr BP (Fig. 3a and legend). The second part of the last deglaciation is more complex and less abrupt than the first, with a 1 °C warming between 11,000 and 7,000 cal. yr BP. Taking into account the dating uncertainties, the warming at ~15,100 cal. yr BP is in phase with that of

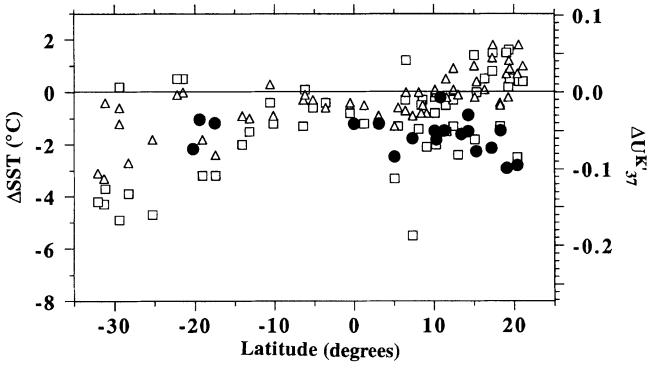


**Figure 2** Mean SST and $U^{K'}_{37}$ differences between LGM and modern for Indian Ocean cores (calibration from ref. 19). Filled circles represent estimates based on the alkenone method applied to 19 high-sedimentation-rate cores from the Indian Ocean (usually >10 cm kyr$^{-1}$). Details will be published elsewhere (C.S. *et al.*, manuscript in preparation). Open squares have been calculated by the TF technique and open triangles by the MAT technique (see text; results described in ref. 5).

Greenland at ~14,900 cal. yr BP (ref. 31). There is also a clear synchrony between the transient feature between 12,200 and 11,500 cal. yr BP and the Younger Dryas cold period observed in the Northern Hemisphere (see, for example, ref. 11). The main difference is that the reversal in core MD79257 does not correspond to a return to full glacial conditions as is the case for the Greenland records (see Fig. 3b).

The temperature reversal at 20° S is similar in relative amplitude to that observed in climate records from Antarctica but the oceanic warming steps are distinctly younger (Fig. 3c). Indeed, the well dated[12,13] isotopic record of the Byrd ice core (West Antarctica) clearly shows that the deglacial warming started at ~20,000–19,000 cal. yr BP, which is much earlier (by ~5,000–4,000 yr) than in core MD79257. Moreover, the second warming which follows the Antarctic Cold Reversal[12–14] leads by ~2,000 yr the second SST increase at 20 °S in the Indian Ocean. Finally, the Holocene temperature optimum in Antarctica is reached at ~9,000–10,000 cal. yr BP, about 3,000 yr before the Holocene SST maximum in core MD79257.

For the time interval between 45,000 and 20,000 cal. yr BP, the $U^{K'}_{37}$ record of MD79257 exhibits a general cooling of ~2 °C. In addition, the $U^{K'}_{37}$ profile shows several warm transients superimposed on the cooling trend, although these are very close to the precision limit. It is tempting to correlate these wiggles with the interstadial warm events recorded in the GRIP ice core (Fig. 3b). These so-called Dansgaard–Oeschger events are of very large magnitude in Greenland (~10 °C with the new $\delta^{18}$O-temperature calibration[17]) and their equivalents in MD79257 are severely attenuated by an order of magnitude. It should also be noted that the warm transients are concomitant with maxima of atmospheric methane concentration[32] measured in air bubbles enclosed in the GRIP ice core (arrows on Fig. 3b).

The recent studies based on terrestrial evidence of mountain glacier readvance in New Zealand[33] and Chile[34] also suggested a climatic synchrony between Southern and Northern hemispheres. Although the dating precision of the New Zealand study was recently criticized[35], our temperature record at 20° S clearly reinforces those previous works and suggests that the synchrony applied to the surface ocean. These observations may be used to discriminate between the climatic mechanisms invoked to explain the timing of the last deglaciation and the abruptness of Dansgaard–Oeschger events.

In particular, rapid variations of global sea level and associated changes of land albedo can be ruled out as explanations of the

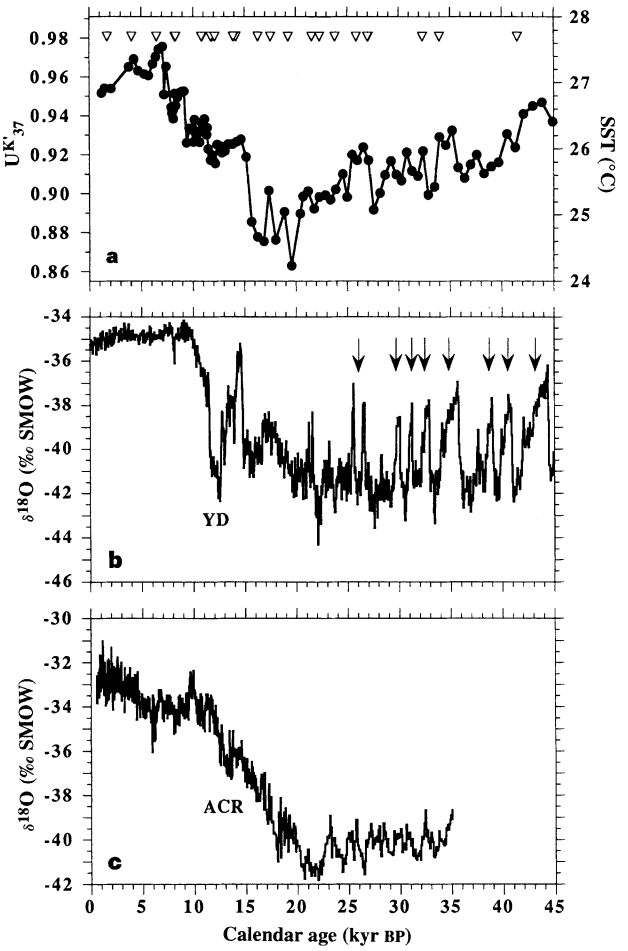


**Figure 3 a**, Alkenone record obtained for core MD79257. $U^{K'}_{37}$ axis is on the left while SST is provided on the right axis (calibration from ref. 19). Open triangles indicate the age control points which are based on AMS-$^{14}$C dating of *Globigerinoides ruber*[29]. For calibrating $^{14}$C ages back to 42 kyr BP we use the following equation based on U-Th dating of corals[30]: age cal. yr BP = $-1{,}807 + 1.39 \times (^{14}\text{C age yr BP}) - 5.85 \times 10^{-6} \times (^{14}\text{C age yr BP})^2$. The calendar timescale for core MD79257 has been obtained by polynomial fitting (fifth-order) through the calibrated AMS-$^{14}$C ages. **b**, $\delta^{18}$O of the GRIP ice core from Greenland[11] with an updated chronology[31]. The arrows indicate the midpoints of the interstadial maxima of atmospheric methane[32]. YD, Younger Dryas period. **c**, $\delta^{18}$O record of the Byrd ice core[39] with an updated chronology[12,13]. ACR, Antarctic Cold Reversal. The midpoint of the 1.5 °C warming step on **a** occurs at the depth level 559 cm in core MD79257 (bracketed between $U^{K'}_{37}$ measurements at 554 and 564 cm). The nearest AMS-$^{14}$C ages are 11,900 ± 210 $^{14}$C yr BP at 540 cm and 13,830 ± 230 $^{14}$C yr BP at 580 cm (ref. 29) which translate into calendar estimates of ~13,900 and ~16,300 cal. yr BP, respectively (ref. 30). The midpoint of this climate warming is thus dated at ~15,100 cal. yr BP.

timing of the last deglaciation. Indeed, ~80% of the deglacial sea level change occurred after 14,200 cal. yr BP as reconstructed by U–Th dating of submerged corals[36]. It thus appears that global sea levels lag behind the deglacial warming observed at different latitudes.

Switching on and off the global thermohaline circulation has been called on to explain warming and cooling events observed in the Northern Hemisphere and, especially, in the North Atlantic area. Numerical modelling of the ocean–atmosphere coupled system suggests that Northern and Southern Hemisphere temperatures should have changed in opposite directions if oscillations of the thermohaline circulation did control the timing of the last deglaciation and Dansgaard–Oeschger events[15,16]. In particular, several models predict a warming for most of the Southern Hemisphere

when the thermohaline circulation is forced to diminish in order to simulate an intense Younger Dryas-type cold event in the North Atlantic area[15,16]. This scenario found some support in the timing of the last deglaciation: the Antarctic Cold Reversal is in phase with the Bølling–Allerød warm period and the second Antarctic warming step corresponds to the Younger Dryas cold event[12–14]. However, the terrestrial data on glacier readvance and our oceanic palaeotemperatures indicate interhemispheric synchrony, reinforcing doubts that the global ocean circulation is the direct and only cause of the climate teleconnection. In fact, as hypothesized recently by Broecker[1], the ocean circulation could have an indirect effect on the Southern Hemisphere by changing the dynamics of the low-latitude atmosphere which in turn would affect the atmospheric water vapour content and hence the strength of its greenhouse effect. The water vapour could act as the rapid vector of interhemispheric teleconnection because low-latitude moisture is redistributed rapidly by large-scale eddies and the mean meridional circulation of the atmosphere[37]. According to Broecker[1], this mechanism could also explain why the break in climate synchrony was at the Antarctic convergence instead of at the Equator. Furthermore, the apparent correlation between atmospheric methane levels and interstadial events would be a logical consequence of this mechanism because low-latitude moisture and temperature fluctuations play major roles in changes of the methane cycle. □

Received 2 September 1996; accepted 14 January 1997.


1. Broecker, W. S. *Geotimes* **41**(2), 40–41 (1996).
2. Webster, P. J. & Streten, N. A. *Quat. Res.* **10,** 279–309 (1978).
3. Guilderson, T. P., Fairbanks, R. G. & Rubenstone, J. L. *Science* **263,** 663–665 (1994).
4. CLIMAP Project Members *Map and Chart Ser. C36* (Geol. Soc. Am., Boulder, 1981).
5. Prell, W. L. *Tech. Rep. TRO25* (Dept of Energy, Washington DC, 1985).
6. Anderson, D. M., Prell, W. L. & Barratt, N. J. *Paleoceanography* **4,** 615–627 (1989).
7. Broecker, W. S. *Quat. Res.* **26,** 121–134 (1986).
8. Stott, L. D. & Tang, C. M. *Paleoceanography* **11,** 37–56 (1996).
9. Brassell, S. C., Eglinton, G., Marlowe, L. T., Pflaumann, U. & Sarnthein, M. *Nature* **320,** 129–133 (1986).
10. Prahl, F. G. & Wakeham, S. G. *Nature* **330,** 367–369 (1987).
11. Johnsen, S. J. *et al. Nature* **359,** 311–313 (1992).
12. Sowers, T. & Bender, M. *Science* **269,** 210–214 (1995).
13. Hammer, C. U., Clausen, H. B. & Langway, C. C. *Ann. Glaciol.* **20,** 115–120 (1994).
14. Jouzel, J. *et al. Clim. Dyn.* **11,** 151–161 (1995).
15. Mikolajewicz, U. *A Meltwater Induced Collapse of the 'Conveyor Belt'* 1–25 (Rep. 189, Max-Planck-Inst. für Meteorol., Hamburg, 1996).
16. Stocker, T. F. & Wright, D. G. *Paleoceanography* **11,** 773–795 (1996).
17. Johnsen, S. J., Dahl-Jensen, D., Dansgaard, W. & Gunderstrup, N. *Tellus* **47B,** 624–629 (1995).
18. Sonzogni, C. *et al. Quat. Res.* (in the press).
19. Prahl, F. G., Muehlhausen, L. A. & Zahnle, D. *Geochim. Cosmochim. Acta* **52,** 2303–2310 (1988).
20. Prahl, F. G., Pisias, N., Sparrow, M. A. & Sabin, A. *Paleoceanography* **10,** 763–773 (1995).
21. Volkman, J. K., Barrett, S. M., Blackburn, S. I. & Sikes, E. L. *Geochim. Cosmochim. Acta* **59,** 513–520 (1995).
22. Sikes, E. L., Farrington, J. W. & Keigwin, L. D. *Earth Planet. Sci. Lett.* **104,** 34–47 (1991).
23. Rosell-Melé, A., Eglinton, G., Pflaumann, U. & Sartthein, M. *Geochim. Cosmochim. Acta* **59,** 3099–3107 (1995).
24. Shackleton, N. J., Hall, M. A., Pate, D., Meynadier, L. & Valet, P. *Paleoceanography* **8,** 141–148 (1993).
25. Meynadier, L., Valet, J. P., Weeks, R., Shackleton, N. J. & Lee Hagee, V. *Earth Planet Sci. Lett.* **114,** 39–57 (1992).
26. Vergnaud Grazzini, C., Caulet, J. P. & Vénec-Peyré, M.-T. *Bull. Soc. Géol. Fr.* **166,** 259–270 (1995).
27. Jouzel, J. *et al. Nature* **364,** 407–412 (1993).
28. Duplessy, J. C., Bé, A. W. H. & Blanc, P. L. *Palaeogeogr. Palaeoclimatol. Palaeoecol.* **33,** 9–46 (1981).
29. Duplessy, J. C. *et al. Earth Planet. Sci. Lett.* **103,** 27–40 (1991).
30. Bard, E., Arnold, M., Fairbanks, R. G. & Hamelin, B. *Radiocarbon* **35,** 191–199 (1993).
31. Hammer, C. U. *et al. The Stratigraphic Dating of the GRIP Ice Core* (Rep. 1 Niels Bohr Inst., Copenhagen, in the press).
32. Chappellaz, J. *et al. Nature* **366,** 443–445 (1993).
33. Denton, G. H. & Hendy, C. H. *Science* **264,** 1434–1437 (1994).
34. Lowell, T. V. *et al. Science* **269,** 1541–1549 (1995).
35. Mabin, M. C. G. *Science* **271,** 668–670 (1996).
36. Bard, E. *et al. Nature* **382,** 241–244 (1996).
37. Del Genio, A., Lacis, A. A. & Ruedy, R. A. *Nature* **351,** 382–385 (1991).
38. Waelbroeck, C. *et al. Clim. Dyn.* **12,** 113–123 (1995).
39. Johnsen, S. J., Dansgaard, W., Clausen, H. B. & Langway, C. C. *Nature* **235,** 429–434 (1972).


**Acknowledgements.** We thank G. Eglinton, J. R. Maxwell, P. J. Müller, T. Rosell-Melé, L. Sikes and J. Volkman for showing us analytical procedures and/or providing alkenone calibration samples; J. P. Caulet, J. C. Duplessy, L. Labeyrie and Y. Lancelot for giving access to cores stored at MNHN in Paris, CFR at Gif-sur-Yvette, and CEREGE in Aix-en-Provence; S. J. Johnsen and J. Jouzel for providing the numerical isotopic data of GRIP, Byrd and Vostok ice cores; M. Arnold, M. Bender, T. Blunier, J. Chappellaz, C. U. Hammer, S. J. Johnsen, J. Jouzel and T. Sowers for comments and help to construct updated chronologies for MD79257, GRIP, Byrd and Vostok cores; L. Beaufort, J. O. Grimalt, G. Haddad, J. Jouzel, U. Mikolajewicz, T. Stocker and T. Webb for discussions and/or reviews of the manuscript; and F. Prahl for comments. This work was supported by MENESR (JE192 and IUF) and INSU (PNEDC).

Correspondence should be addressed to E.B. (e-mail: ebard@arbois.cerege.fr).

# Direct observation of complete miscibility in the albite–$H_2O$ system

**Andy H. Shen* & Hans Keppler†**

* *Department of Earth Sciences, University of Cambridge, Downing Street, Cambridge CB2 3EQ, UK*

† *Bayerisches Geoinstitut, Universität Bayreuth, 95440 Bayreuth, Germany*

**There are essentially two main types of mobile phases in the Earth's crust and mantle: silicate melts and hydrous fluids. Near the surface of the Earth, the physical and chemical properties of these phases are fundamentally different. But with increasing pressure, the solubility of water in silicate melts and the solubility of silicate materials in hydrous fluids increase. This has led to the suggestion that, above a certain critical pressure, the compositions of the two phases in mutual equilibrium become indistinguishable[1–5]. Here we report the direct visual observation of this phenomenon in the albite–$H_2O$ system using an externally heated diamond anvil cell. Our results suggest both that there should be complete miscibility between silicate melts and hydrous fluids in the deeper parts of the upper mantle and that, in the presence of a hydrous fluid, a melting temperature for this part of the mantle can no longer be defined.**

In our experiments, we used a Bassett-type externally heated diamond anvil cell[6,7]. In this cell, the sample is contained in a 500-μm borehole in a rhenium gasket with an initial thickness of 250 μm. The gasket is compressed between two flat diamond surfaces of 1 mm diameter. Heating is achieved by electrical coils around the tungsten carbide seats below the diamond and temperature is measured by an external thermocouple touching the diamonds. It has been shown that after cycling the cell a few times through the temperature interval of interest, it behaves as an isochoric system[8]. If water is used as a pressure medium, the pressure at any temperature inside the cell may be determined from the equation of state of water, provided the bulk density of the fluid phase in the cell is known[8]. This can easily be determined by measuring the melting temperature of ice in the cell or the temperature at which a vapour bubble disappears in the cell on heating.

At the beginning of each experiment, we filled the cell with water to the desired bulk density and cycled it several times through the temperature interval of interest. We then opened the cell again and filled it with about equal amounts by weight of water and hydrous albite glass ($NaAlSi_3O_8$, containing 5 wt% of $H_2O$). On heating above the glass transformation temperature, a round drop of hydrous silicate melt forms which is surrounded by water, containing some dissolved silicate material (Fig. 1a). If the temperature and pressure inside the cell approaches a critical point, the compositions of the two phases converge. This results in a reduced optical contrast between the two phases and fading of the phase boundary (Fig. 1b and c). At the critical point, the phase boundary disappears entirely (Fig. 1d). Note that this critical behaviour is very different from the simple dissolution of a phase. If a phase dissolves, its composition remains constant but its volume decreases. In a system with critical behaviour, the compositions of the respective phases change, while their volumes remain approximately constant. When the homogeneous, supercritical phase in the diamond cell was cooled again to a temperature a few °C below the critical homogenization temperature observed on heating, it first turned milky and then separated into a fluid phase and a melt phase. During this process, vigorous turbulence was observed inside the sample chamber. The milky appearance of the sample just before phase separation is a typical